Numerical lifting line theory for a hydrofoil near a free surface

G.D.Thiart[1]

Abstract

A numerical lifting line theory for the calculation of lift on a hydrofoil of finite span near a free surface is presented. Nonlinearities in the lift curve slope of the hydrofoil sections are accounted for, and a downwash correction due to the presence of the free surface is also included. Theoretical results are compared with experimental results for a 5.11 aspect ratio hydrofoil of the circular arc type. The lift curves of the hydrofoil sections as function of depth of submergence and angle of attack were calculated by means of a linearized free surface boundary condition panel method. These section lift curves were used to calculate the finite span hydrofoil lift curves by means of the numerical lifting line theory. The theoretical results compare favourably with the experimental results, and it is shown that much better agreement between theory and experiment is obtained as compared to results obtained with a simple aspect ratio correction factor based on Prandtl's lifting line theory.

Nomenclature

a_k, b_k, c_k	constants in quadratic curve fit
A_R	hydrofoil aspect ratio (s^2/plan areas)
c	hydrofoil section chord
C_{D_i}	induced drag coefficient
C_l, C_L	section lift coefficient, hydrofoil lift coefficient
F'	force per unit length
Fr	Froude number
g	acceleration of gravity
h, h_{te}	depth of submergence of lifting line, depth of submergence of trailing edge
k	index
N	number of panels, hydrofoil sections
s	hydrofoil span
t	maximum thickness of hydrofoil
x, y, z	coordinates in free stream direction, along hydrofoil span, perpendicular to undisturbed free surface
u, w	velocity components in x-direction, z-direction
V_∞, V_e	free stream velocity, effective velocity at lifting line
w_i	downwash at lifting line induced by trailing vorticity
$\alpha, \alpha_0, \alpha_e$	geometrical angle of attack, zero-lift angle, effective angle of attack at hydrofoil section
γ	strength of trailing vorticity
Γ	circulation
η	dummy variable in spanwise direction
ϕ_w	wave-making velocity potential
ρ	fluid density

Introduction

The calculation of the lift generated by a hydrofoil near a free surface is necessary for the determination of the performance of hydrofoil supported craft such as hydrofoil boats supported by surface-piercing struts or hydrofoil supported catamarans. There are a number of methods available for the calculation of the lift of a hydrofoil of infinite length beneath a free surface, e.g. the thin hydrofoil theory of Hough & Moran [1] and the panel method of Giesing & Smith.[2] Both of these methods are based on the linearized free surface boundary condition applied at the undisturbed free surface. A number of calculation methods which employ the exact nonlinear free surface boundary condition at the exact location of the free surface have also been presented recently.[3–6]

The calculation of the lift of a hydrofoil of finite length beneath a free surface has received much less attention. Current practice usually involves the correction of two-dimensional results by means of Prandtl's lifting line theory [7;8] or other more elaborate correction formulas.[9]

The purpose of this paper is to present the numerical lifting line theory for hydrofoils of finite span near a free surface. The method of calculation is similar to that of Anderson *et al.* [10] in that the nonlinear lift curve slope (with respect to angle of attack) of the hydrofoil section is accounted for, but a more sophisticated approach towards the calculation of the improper integrals that arise in the formulation is adopted. Furthermore, a correction due to the presence of the free surface is included in the present theory.

The theory is applied to a 5.11 aspect ratio hydrofoil which is very similar to a Göttingen K11 profile, and the results are compared with experimental data. It is shown that better agreement between theory and experiment is

[1]Senior lecturer, Department of Mechanical Engineering, University of Stellenbosch, Stellenbosch, 7600 Republic of South Africa

obtained compared to the case when a simple aspect ratio correction factor based on Prandtl's lifting line theory is utilized.

Theoretical model

The basis of the lifting line model [10] is the postulate that straight wings of large aspect ratio may be represented by a single bound vortex line at the quarter-chord. The strength of this vortex line (the lifting line) varies along the span, with the local strength given by the circulation $\Gamma(y)$. A trailing vortex is generated at each point on the wing where the circulation changes, the strength of the trailing vortex being equal to the change in circulation at the point where it leaves the lifting line. For a continuous circulation distribution, the strength of the trailing vortex starting at a given point on the lifting line is given by $\gamma(y) = d\Gamma / dy$.

A further postulate is that local value of circulation may be related to the local force per unit span F' by means of a modified version of the Kutta-Joukowski theorem,

$$F'(y) = \rho V_e(y)\Gamma(y) \tag{1}$$

Here V_e is the local effective velocity 'seen' by the lifting line, composed of the free stream velocity V_∞ and the downwash velocity w_i induced by the trailing vortex sheet:

$$V_e = \sqrt{V_\infty^2 + w_i^2} \tag{2}$$

The effective angle of attack is given by

$$\alpha_e(y) = \alpha - \alpha_0 - \arctan(w_i / V_\infty) \tag{3}$$

where α is the geometrical angle of attack and α_0 the zero-lift angle.

The direction of F' is perpendicular to the direction of V_e, and its value may be found from

$$F'(y) = \frac{1}{2}\rho V_e^2(y) c(y) C_1(\alpha_e) \tag{4}$$

where c is the local section chord, and C_1 is the local (two-dimensional) section lift coefficient which is a function only of the local effective angle of attack $\alpha_e(y)$. It follows, from equations (1) and (4), that

$$\Gamma(y) = \frac{1}{2} V_e(y)\, c(y)\, C_1(\alpha_e) \tag{5}$$

In the presence of a free surface the downwash distribution depends not only on the circulation distribution on the hydrofoil, but also on gravity effects. The effect of the free surface may be accounted for via the linearized free-surface boundary condition applied at the undisturbed free surface:[1;2]

$$\frac{\partial u}{\partial x} + \frac{g}{V_\infty^2} w = 0 \quad \text{at } z = 0 \tag{6}$$

The velocity field induced by the bound vortex and the trailing vortex sheet has to be augmented so that this boundary condition in satisfied. Two other conditions that also have to be satisfied are the radiation condition, i.e. that the free surface remains undisturbed far ahead of the hydrofoil, and the depth condition, i.e. no disturbances very far below the hydrofoil. This may be achieved by means of the image in the plane $z = 0$ of the bound lifting line and its associated trailing vortex sheet, plus a so-called wave-making velocity potential ϕ_w. All gravity effects are included in this wave-making potential, which has to be a solution of Laplace's equation, i.e. $\nabla^2\phi_w = 0$.

Application of the law of Biot-Savart to the trailing vortex sheet and its image leads to the following equation for the downwash at the lifting line of length s situated at depth h beneath the undisturbed free surface:

$$\begin{aligned} w_i(y) = {} & \tfrac{1}{4\pi}\int_{-s/2}^{s/2} \tfrac{d\Gamma}{d\eta}\tfrac{1}{y-\eta}\, d\eta \\ & -\tfrac{1}{4\pi}\int_{-s/2}^{s/2} \tfrac{d\Gamma}{d\eta}\tfrac{y-\eta}{4h^2+(y-\eta)^2}\, d\eta \end{aligned} \tag{7}$$

The first term is the downwash due to the trailing vortex sheet at the lifting line, and the second term (without the minus sign) the upwash due to the image trailing vortex sheet.

The trailing vortex sheet and its image satisfy equation (6), the linearized free surface boundary condition, exactly, because both the axial velocity component u and the vertical velocity component w induced by the two sheets are zero everywhere on $z = 0$. It can therefore be consluded that the wave-making velocity potential associated with the trailing vortex sheet is exactly zero, and hence that wave-making effects are introduced only via the two-dimensional calculation procedure for determining the section lift characteristics.

In the classical lifting line theory, V_e is assumed to be equal to the free stream velocity, C_1 is assumed to be a linear function of α_e, and $\arctan(w_i / V_\infty)$ in equation (3) is replaced by w_i / V_∞ under the assumption that the magnitude of the downwash is small compared to the magnitude of the free stream velocity. This leads to Prandtl's integro-differential equation with $\Gamma(y)$ as the only unknown [11], which can be solved by means of Fourier analysis. In the present paper, the methodology of Anderson *et al.* [10] is used to solve the problem numerically, which obviates the need for the three assumptions leading to Prandtl's equation. According to this methodology, $C_1(\alpha_e)$ is determined by means of an appropriate two-dimensional calculation method or from experimental data, whereafter equations (2), (3), (5), and (7) are solved iteratively. An appropriate circulation distribution, e.g. elliptical or calculated by means of Prandtl'sequation, is used to start the iteration process.

For the purposes of this paper, it is assumed that the spanwise lift distribution is symmetrical, i.e. $\Gamma(y) = \Gamma(-y)$; the procedure for a nonsymmetrical lift distribution is similar. The wing is subdivided into N spanwise sections, and a quadratic variation in circulation is assumed to exist over every section, i.e.

$$\Gamma(y) = a_k + b_k y + c_k y^2; \quad k = 1, \ldots N; \quad y_{k-1} \le y \le y_k \tag{8}$$

with $y_0 = 0$. The quadratic variation is necessary to ensure that the first integral in equation (7) can be determined analytically; the coefficients a_k, b_k and c_k for each section are determined from the known values of Γ_k determined at the previous iteration, and the requirements that $d\Gamma / dy = 0$ at y_0, and that $d\Gamma / dy$ be continuous between adjacent sections.

Substitution of equation (8) into equation (7) yields the following discretized expression for the downwash at the lifting line:

$$w_i(y) = \frac{1}{4\pi} \sum_{k=1}^{N} \int_{y_{k-1}}^{y_k} (b_k + 2c_k\eta) \times \left[\frac{1}{y-\eta} - \frac{1}{y+\eta} - \frac{y-\eta}{4h^2+(y-\eta)^2} + \frac{y+\eta}{4h^2+(y+\eta)^2} \right] d\eta \quad (9)$$

The integral of the first two terms in equation (9), representing the downwash due to the vortex sheet, is as follows:

$$\int_{y_{k-1}}^{y_k} (b_k + 2c_k\eta) \left[\frac{1}{y-\eta} - \frac{1}{y+\eta} \right] d\eta = b_k \ln \left| \frac{(y-y_{k-1})(y+y_{k-1})}{(y-y_k)(y+y_k)} \right| + 2c_k y \ln \left| \frac{(y-y_{k-1})(y+y_k)}{(y+y_{k-1})(y-y_k)} \right| - 4c_k (y_k - y_{k-1}) \quad (10)$$

If $y = y_k$ (or $y = y_{k-1}$), the integrals have to be evaluated in the Cauchy principle value sense; it can be shown that the factor $y - y_k$ (or $y - y_{k-1}$, as appropriate) can then simply be omitted from equation (10), or replaced by a constant such as h or s to ensure that the arguments of the logarithmic terms remain non-dimensional.

The integral of the second two terms in equation (9), representing the downwash due to the image of the trailing vortex sheet, is given by

$$\int_{y_{k-1}}^{y_k} (b_k + 2c_k\eta) \left[-\frac{y-\eta}{4h^2+(y-\eta)^2} + \frac{y+\eta}{4h^2+(y+\eta)^2} \right] d\eta = \frac{1}{2} b_k \ln \left| \frac{\{4h^2+(y-y_k)^2\}\{4h^2+(y+y_k)^2\}}{\{4h^2+(y-y_{k-1})^2\}\{4h^2+(y+y_{k-1})^2\}} \right| + c_k y \ln \left| \frac{\{4h^2+(y+y_{k-1})^2\}\{4h^2+(y-y_k)^2\}}{\{4h^2+(y-y_{k-1})^2\}\{4h^2+(y+y_k)^2\}} \right| + 4c_k h \left[\begin{array}{l} \tan^{-1} \frac{y-y_k}{2h} - \tan^{-1} \frac{y-y_{k-1}}{2h} \\ -\tan^{-1} \frac{y+y_k}{2h} + \tan^{-1} \frac{y+y_{k-1}}{2h} \end{array} \right] + 4c_k (y_k - y_{k-1}) \quad (11)$$

The method of numerical integration of the downwash integrals presented here differs substantially from that of Anderson *et al.*, who used Simpson's rule and approximated the singular cases ($y = y_k$) as the average of the integrals for adjacent sections.

After a converged solution for the circulation distribution has been obtained, the lift and induced drag coefficients of the hydrofoil can be computed in the usual manner:

$$C_L = \frac{2A_R}{V_\infty s^2} \int_{-s/2}^{s/2} \Gamma(y)\, dy \quad (12)$$

$$C_{D_i} = \frac{2A_R}{V_\infty^2 s^2} \int_{-s/2}^{s/2} w_i(y)\, \Gamma(y)\, dy \quad (13)$$

Equation (12) is evaluated by utilizing the quadratic curve fits of equation (8), and equation (13) in a similar manner by assuming that the product $w_i(y)\Gamma(y)$ also varies quadratically over every section.

Comparison with experiment

For the purpose of comparison, experimental data for a 5.11 aspect ratio hydrofoil that was measured in the University of Stellenbosch towing tank [6] were selected. The foil section is very similar to a Göttingen K11 profile: it has a flat pressure side, a circular arc suction side, and a leading edge radius equal to $0.970t^2/c$, where t is the maximum thickness of the profile. The maximum thickness of the tested profile was equal to $0.077c$ compared to the maximum thickness of $0.075c$ for the Göttingen K11 profile.

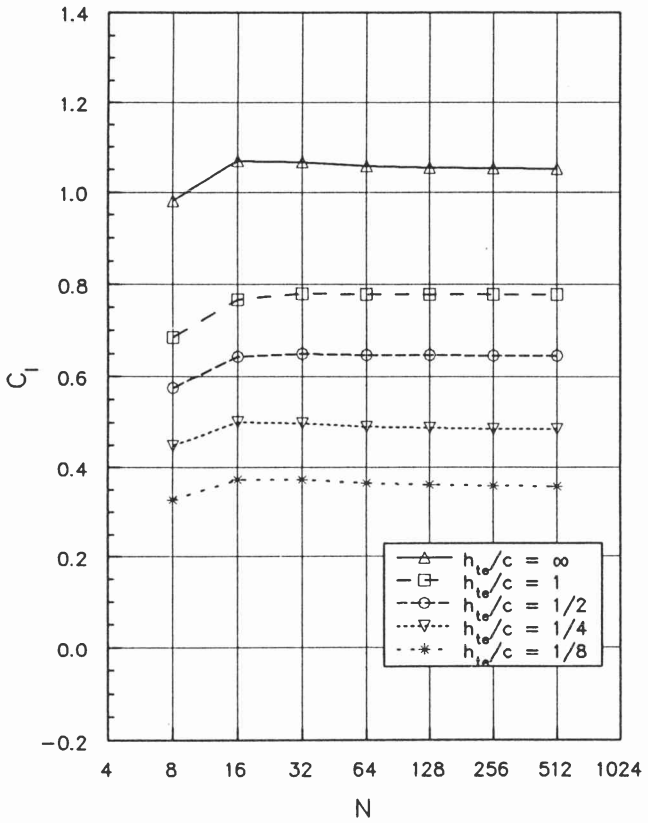

Figure 1 Convergence of section lift coefficients for $\alpha = 4.5°$

The section lift characteristics for the chosen section was calculated by means of the panel method of Giesing & Smith,[2] implemented in FORTRAN 77 on a 486 personal computer. The panels were distributed over the chord of the section according to the well-known semicircle method, except on the rounded leading edge, where panels of equal length were used. The lift characteristicswere calculated for a Froude number $Fr = V_\infty / \sqrt{(gc)}$ of 4.3, depth of submergence of the trailing edge h_{te} equal

to 1/8, 1/4, 1/2, and 1 times chord length, and angles of attack ranging from −4.5° to 6°, corresponding to the towing test conditions. The lift curve for infinite submergence was also calculated. In order to ascertain whether the results were independent of panel size, the number of panels was varied from 2^3 (8 panels) to 2^9 (512 panels) for every case. The typical convergence behaviour of the section lift coefficient as function of the number of panels is illustrated in Figure 1 for $\alpha = 4.5°$. It took approximately 6 min of CPU time to calculate one data point for 512 panels.

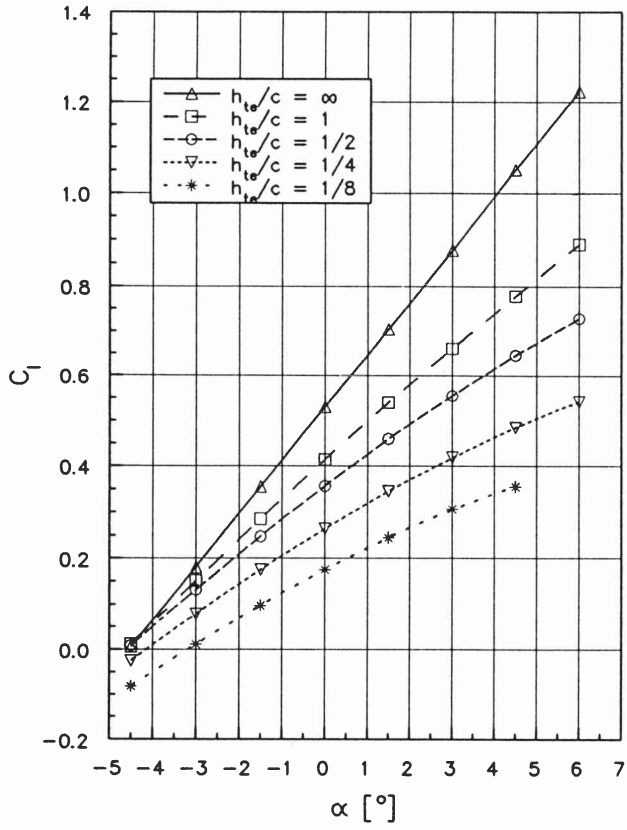

Figure 2 Calculated section lift characteristics (symbols represent calculated points, lines represent quadratic curve fits)

The results were extrapolated to zero panel size by means of Richardson [12] extrapolation; it is estimated that these extrapolated values should generally be accurate to four decimal figures compared to the exact (but unknown) potential flow solution. The calculated section lift characteristics are shown in Figure 2 (the method of Giesing & Smith can only be applied if the hydrofoil is completely submerged beneath the undisturbed free surface; for the trailing edge depth of $c/8$ this corresponds to a maximum angle of attack of approximately 4.5°), together with their corresponding quadratic least squares curve fits. It is clear that the characteristics as calculated can be approximated by quadratic polynomials to a high degree of accuracy. The coefficients of these curve fits are presented in Table 1.

Table 1 Quadratic curve fit coefficients for C_l

Coefficient of	α^0	α^1 [rad^{-1}]	α^2 [rad^{-2}]
$h_{te} = \infty$	0.5296889	6.645067	−0.306030
$h_{te} = c$	0.4146372	4.876007	−3.159077
$h_{te} = c/2$	0.3562194	4.048844	−4.674135
$h_{te} = c/4$	0.2635960	3.243845	−5.480603
$h_{te} = c/8$	0.1750660	2.796657	−6.162090

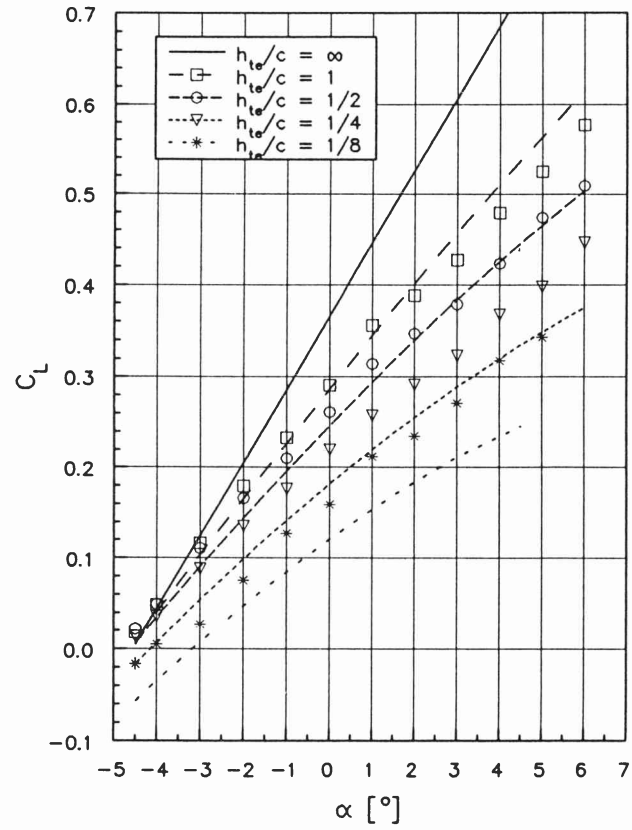

Figure 3 Comparison of experimental lift characteristics with calculated results corrected by means of Prandtl's lifting line theory (symbols represent experimental results, lines represent numerical results)

The correction factor for a 5.11 aspect ratio rectangular flat plate as calculated by means of Prandtl's lifting line theory was found to be equal to 0.6909. The experimental lift curves are compared in Figure 3 with the calculated two-dimensional results multiplied by this correction factor. For $h_{te}/c = 1$, the experimental values are underestimated at small angles of attack (up to about 1°), but for larger angles the experimental values are overestimated. The reason for this dualistic behaviour is that there is a modest discontinuity in the slope of the measured lift curve at about $\alpha = 1$, which can probably be ascribed to leading-edge separation of the long bubble type as described by Hoerner & Borst.[13] The potential

flow theory used to calculate the section lift coefficients of course does not make provision for separated flow. The same comments apply in principle for the comparison at $h_{te}/c = 1/2$. For $h_{te}/c = 1/4$ and $1/8$, correspondence between theory and experiment is poor: the theory underestimates the lift by a considerable margin.

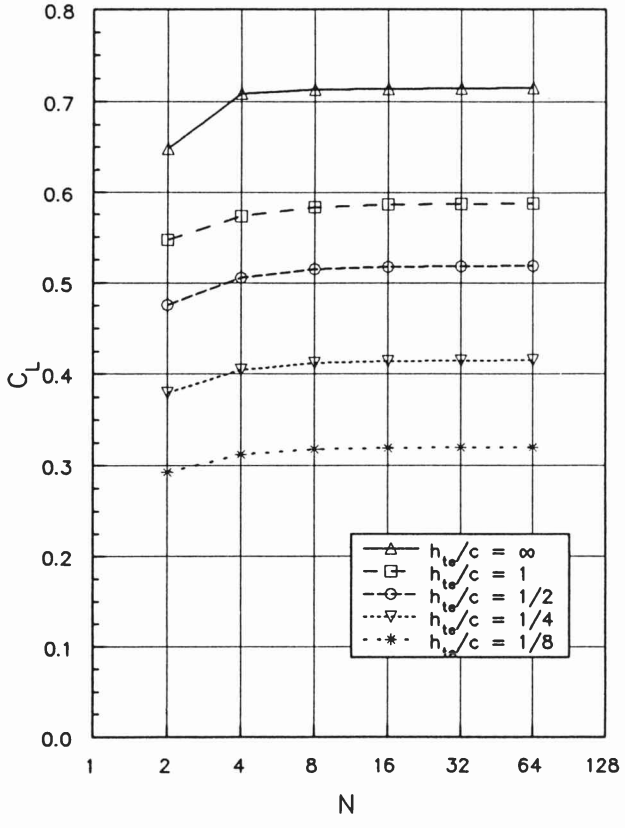

Figure 4 Convergence of hydrofoil lift coefficients for $\alpha = 4.5°$

The numerical lifting line theory, utilizing the section lift characteristics as defined in Table 1, was also implemented in FORTRAN 77 on the 486 personal computer. Sections along the hydrofoil span were distributed according to the semi-circle method, and calculations were performed for the number of sections ranging from 2 to 2^6 (64). The typical convergence behaviour of the hydrofoil lift coefficient as function of number of sections is illustrated in Figure 4, also for $\alpha = 4.5°$. The CPU time required for one 64-section data point is about 30 s, involving approximately 40 iterations with a relaxation factor of 0.05 on downwash and circulation. It is estimated that the 64-section results should generally be accurate to three decimal figures.

The 64-section results are compared with the experimental results in Figure 5. For $h_{te}/c = 1$ and $1/2$, the experimental values are fairly well predicted up to about $\alpha = 1°$, where the discontinuities in the experimental lift curves are located. For $h_{te}/c = 1/4$ and $1/8$, correspondence between theory and experiment is also much improved relative to the theoretical results based on the Prandtl lifting line correction factor.

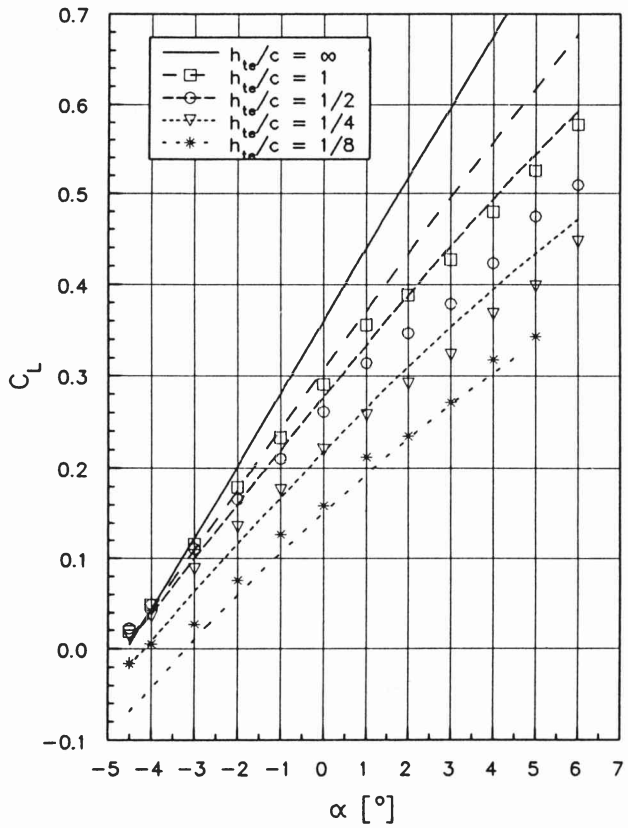

Figure 5 Comparison of experimental lift characteristics with numerical lifting line theory (symbols represent experimental results, lines represent numerical results)

Conclusions

A method for calculating the lift on a hydrofoil near a free surface has been presented. It was demonstrated that the lift on a circular arc hydrofoil of finite span near a free surface can be predicted fairly well for small angles of attack by means of this theory. There is scope for further improvement by accounting for viscous effects in the two-dimensional calculation procedure.

Induced drag can also be calculated by means of the method, but, since induced drag cannot be measured separately from other major contributions such as viscous and wave drag, no comparison with experimental drag results was presented. The prediction of the drag of a hydrofoil of finite span near a free surface is one of the topics envisaged for further research.

References

[1] Hough GR & Moran JP. Froude number effects on two-dimensional hydrofoils. *J. Ship Res.*, 1969, **13**, pp.53–60.

[2] Giesing JP & Smith AMO. Potential flow about two-dimensional hydrofoils. *J. Fluid Mech.*, 1967, **28**, pp.113–129.

[3] Çalisal SM, Gören O & Okan B. On an iterative solution for nonlinear wave calculations. *J. Ship Res.*, 1991, **35**, pp.9–14.

[4] Chen L & Vorus WS. Application of a vortex method to free surface flows. *Int. J. Num. Meth. Fluids*, 1992, **14**, pp.1289–1310.

[5] Lalli F, Campana E & Bulgarelli U. Numerical simulation of fully nonlinear steady free surface flow. *Int. J. Num. Meth. Fluids*, 1992, **14**, pp.1135–1149.

[6] Von Backström TW, Thiart GD & Hoppe KG. Numerical prediction of the lift of a hydrofoil near a free surface. *Third National Symposium on Computational Fluid Dynamics*, Stellenbosch, 1993.

[7] Johnson RS. Prediction of lift and cavitation characteristics of hydrofoil-strut arrays. *Marine Technology*, 1965, **2**, pp.57–69.

[8] Furuya O. Three-dimensional theory on supercavitating hydrofoils hear a free surface. *J. Fluid Mech.*, 1975, **71**, pp.339–359.

[9] Van Manen JD & Van Oossanen P. High speed craft and advanced marine vehicles. In: Lewis EVL (ed.). *Principles of Naval Architecture*, **3**, p.114. SNAME, Jersey City, 1988.

[10] Anderson JD, Corda S & Van Wie DM. Numerical lifting line theory applied to drooped leading-edge wings below and above stall. *J. Aircr.*, 1980, **17**, pp.898–904.

[11] Kuethe AM & Chow C-Y. *Foundations of aerodynamics*, 3rd edn, Wiley, New York, 1976.

[12] Richardson LF. The approximate arithmetical solution by finite differences of physical problems involving differential equations, with an application to the stresses in a masonry dam. *Trans. Roy. Soc. London*, Ser. A., 1910, **210**, pp.307–357.

[13] Hoerner SF & Borst HV. *Fluid-dynamic lift*, Ch. 4, p.3. Hoerner Fluid Dynamics, Brick Town, New Jersey, 1975.